MEDDOCS Open Access Publisher

ISSN: 2639-9237

Journal of Case Reports and Medical Images

Open Access | Research Article

Prognosis Prediction In NPC Based on Radiomic Models Of F-18 FDG PET/CT Images

Chia Ni Lee[1]; Yi-Ching Lin[2,3,5]MD; He-Yuan Hsieh[4]MD; Jui-Yin Kung[2,3]; Chun Ting Chiang[1]; Jyh-Cheng Chen, PhD[1,6,7]*; Shih-Chuan Tsai[2,3]*MD.

[1]Department of Biomedical Imaging and Radiological Sciences, National Yang Ming Chiao Tung University, Taipei, Taiwan.

[2]Department of Nuclear Medicine, Taichung Veterans General Hospital, Taichung, Taiwan.

[3]Department of Medical Imaging and Radiological Technology, Institute of Radiological Science, Central Taiwan University of Science and Technology, Taiwan.

[4]Department of Radiation Oncology, Taichung Veterans General Hospital, Taichung, Taiwan.

[5]Department of Public Health, China Medical University, Taichung, Taiwan.

[6]Department of Biomedical Imaging and Radiological Science, China Medical University, Taiwan.

[7]School of Medical Imaging, Xuzhou Medical University, Xuzhou 221004, China.

**C.N.L., Y.C.L. and H.Y.H. contributed equally to this work as the joint first authors.*

[#]J.C.C. and S.C.T. contributed equally to this work.

***Corresponding Author(s): Jyh-Cheng Chen[1] & Shih-Chuan Tsai[2]**

[1]Department of Biomedical Imaging and Radiological Sciences, National Yang Ming Chiao Tung University, Taipei, Taiwan.

[2]Department of Nuclear Medicine, Taichung Veterans General Hospital, Taichung, Taiwan.

Emails: jcchen@ym.edu.tw& sctsai@vghtc.gov.tw

Received: Mar 13, 2023

Accepted: Apr 03, 2023

Published Online: Apr 10, 2023

Journal: Journal of Case Reports and Medical Images

Publisher: MedDocs Publishers LLC

Online edition: http://meddocsonline.org/

Abstract

Nasopharyngeal Carcinoma (NPC) is one of the most common head and neck cancers. Positron emission tomography/computed tomography (PET/CT) combines biological metabolic information and anatomical images, and therefore, plays a crucial role in the diagnosis, treatment, and prognosis of NPCs. In this study, however, we aim to diagnose and treat diseases from a macroscopic perspective. Radiomics is a technology that has been used widely in the context of various cancers that involves mining deep information contained in medical images. The aims of this study were to construct radiomic models of NPC staging based on PET/CT images with 2-deoxy-2-[fluorine-18] fluoro-D-glucose (F-18 FDG), to investigate the correlation between metabolic parameters and radiomic features and to provide prognostic predictions.

Materials and Methods: We retrospectively collected data from 103 patients with NPC from Jan. 2010 to Dec. 2020. Throughout pre-treatment staging and post-treatment follow-up for treatment effectiveness, each subject had at least three F-18 FDG PET/CT images performed. Metabolic parameters and standardized uptake values (SUVs), of the local NPC lesions were measured. Radiomic features were extracted from the PET image via PyRadiomics. A total of 107 radiomic features based on the PET/CT images were calculated. The relationships between the metabolic parameters and radiomic features were analyzed via a Pear-

Cite this article: Chia-Ni L, Yi-Ching L, Jyh-Cheng C, Shih-Chuan T. Prognosis Prediction In NPC Based On Radiomic Models Of F-18 FDG PET/CT Images. J Case Rep Clin Images. 2023: 6(1): 1136.

son's correlation analysis and subsequent generation of a heatmap. Support vector machine (SVM) classification was performed to identify the feature combinations that most frequently achieved the highest area under the receiver operating characteristic (ROC) curve (AUC) for predicting progression-free survival (PFS).

Results: Compared to SUVs, the radiomic features showed a low relationship in shape, flatness, and some first-order features. The Pearson's correlation analysis showed that the metabolic parameters displayed different degrees of correlation with the selected radiomic features. First, radiomic features displaying low correlation with SUVs were selected and imported into the SVM model, where we then reduced the number of features. For the training group, the accuracy was 74.3%, the sensitivity was 95.9%, and the specificity was 76.2%. For the test group, the accuracy was 58.3%, the sensitivity was 91.7%, and the specificity was 75%.

Conclusion: We found that radiomic feature selection and modeling in PET images can benefit the process of prognosis prediction in NPC. In our future work, we hope to create a prediction model for NPC as well as perform validation of our clinical PET images.

Introduction

Nasopharyngeal Carcinoma (NPC) is one of the most common head and neck cancers. The incidence of NPC varies with respect to region. Globally, NPC is more common in southern China, southeastern Asia, and northern Africa [1-3]. Treatment options and prognoses vary greatly depending on tumor grade and risk assessment of the specific patient. Although advancements in radiotherapy techniques and chemotherapy strategies have improved NPC prognosis, approximately one-third of patients still experience relapse [4-5].

Imaging modalities, such as Computed Tomography (CT), Magnetic Resonance Imaging (MRI), and Positron Emission Tomography (PET), are widely used in the early diagnosis, staging, restaging and treatment response evaluation of NPC. Positron Emission Tomography/Computed Tomography (PET-CT) combines biological metabolic information and anatomical images, and therefore plays a crucial role in the diagnosis, treatment, and prognosis of NPCs. Many studies have reported an association between clinical outcomes and quantitative measurement based on 2-deoxy-2-[fluorine-18] fluoro-D-glucose (F- 18 FDG) PET/CT findings by utilizing parameters such as Standard Uptake Values (SUVs) and metabolic tumor volume [6-8]. However, these applications have been aimed at diagnosing and treating diseases from a macroscopic perspective. Most of these medical images

heterogeneity, which is predictive of prognostic outcomes [9, 10].

Recently, several studies have reported that radiomics can provided extensive amounts of high- dimensional information related to tumor heterogeneity not normally visible to the naked eye, such as tumor cellularity, degenerative changes, and neovascularization [11]. Radiomics refers to the process of extracting quantitative imaging features (radiomic features), describing detailed tumor characteristics, from routine medical images, and has been used widely in the analysis of various cancers. Examples of radiomic features include tumor size, geometry, voxel intensity, and textural patterns. Several studies have shown the potential of radiomic features in the prognostic prediction of many types of cancers, including NPC [12-17].

The purpose of this study was to construct radiomic models of NPC staging based on PET/CT images, to investigate the correlation between metabolic parameters and radiomic features, and to evaluate the prognostic value of radiomics in the assessment of NPC patients.

Methods and Materials

Subjects

In this study, we retrospectively collected data from103 newly diagnosed NPC patients who were admitted between January 1, 2000, and December 31, 2020, at Taichung Veterans General Hospital. Each patient was subjected to at least three FDG PET/CT examinations, including (i) pre-treatment images to establish baseline radiomic values, (ii) post-treatment images to evaluate treatment effectiveness, and (iii) follow-up images to evaluate the effectiveness of follow-up treatment. All patients had no evidence of distant metastasis and did not have any other malignancies. Institutional ethics review board approval was obtained for this study at the Taichung Veterans General Hospital.

Imaging acquisition

All PET/CT scans were performed using a dedicated PET/CT scanner (Gemini TF 16,Philips Healthcare, Cleveland, OH, USA). Imaging was performed using a combination PET/CT scanner according to PET/CT tumor imaging guidelines [23].

After fasting for at least 4 hours (except for glucose-free hydration), blood sugar was measured to confirm a value lower than 200 mg/mL. The scans were performed approximately 1 hour after intravenous injection of F-18 FDG at a dose of 0.1 mCi/kg body weight.

The study was done with patient in supine position, and across the entire body from the base of the skull down to the level of the mid-thigh. With the patient breathing normally, a low-dose CT was performed for attenuation correction, followed by a PET scan.

The parameters of the CT scan were as follows: Tube voltage: 120 kilovolts (kV), tube current: 80 milliamperes (mA), x-ray tube rotation/turn: 0.5 seconds, pitch setting: 0.8266 (pitch=bed travel distance/beam width) and slice thickness: 5 mm.

Additional notable CT scan parameters were as follows: 9-10 beds (according to patient body height), 1 min for each bed position. Images were reconstructed using the ordered subsets expectation method (OSEM) into 3-axis images.

Metabolic parameters and standardized uptake values (SUVs) of the local NPC lesions were measured. The region of interest (ROI) was be selected when the SUV was greater than 2.5. When selecting the ROI, the primary NPC site was set as Local, which is defined as the area of high uptake in the nasopharyngeal region on the PET image **(Figure 1)**. The primary site lymph node, set as Lymph X (where X represents a numerical code), was defined as the area of high lymph node uptake in the head and neck regions on PET images **(Figure 2)**.

Because the patient selection process screened for patients whose baseline scans included distant metastases, an area of high uptake in other regions not listed above was selected as

the ROI.

Region of Interest selection and radiomic features extraction

In this study, 3D Slicer image processing software (software version: 4.10.2) was chosen as the software in whichthe ROI would be drawn. The patients' FDG PET images were loaded into 3D Slicer. The level tracking (adaptive threshold) method was used to semi-automatically draw an ROI, after which a volume of interest (VOI) would be constructed slice by slice. PET Tumor Segmentation was another method of ROI selection, which was capable of performing one-click VOI selection.

Afterwards, the plug-in program PyRadiomics (version PyRadiomics 2.2.0) was used to extract radiomic feature values (texture analysis). SPSS (IBM, Version 24) was then used to calculate the Pearson's correlation. We used the SUV to calculate correlational relationships among the features, after which we created a heatmap to display these correlational relationships. The endpoint was defined as cancer recurrence or the appearance of any metastasis happened, as defined by Progression Free Survival (PFS).

Statistical analysis

Using the default SciPy package, we performed the sign test to compare the radiomic features, and SUVs. The Pearson's correlation method was used to calculate the correlation coefficients for the relationships between the SUV and each radiomic features. The selected features were chosen based on the correlation coefficient between the feature and SUV. Features displaying low correlation coefficients were selected first. All statistical analyses were performed using IBM SPSS version 24.0.

SVM classifier

In terms of machine learning methods, we chose the SVM (Support Vector Machine) classifier for advanced radiomic feature selection. The SVM classifier is a supervised learning method used for classification, regression, and outlier detection. The advantages of SVM in our experiment are, (i) that it is still effective in cases where the number of dimensions is greater than the number of samples, and

(ii) that it is highly memory-efficient, as it uses a subset of training points (called support vectors) in the decision function (24, 25). The disadvantage of SVM in our experiment is that it does not directly

provide probability estimates; these must be calculated using an expensive five-fold cross-validation process.

Results

NPC patient data

The summarized data of all NPC patients are listed in **Table 1**. A total of 103 patients were enrolled, of which 75 were male and 28 were female, resulting in a male-to-female ratio of 2.32:1. 36 patients were classified as non-recurrent the conditions of which mandated no recurrence of the tumor in the primary site, no regional lymph node metastases and no post-treatment distant metastases. 67 patients presented with some type of recurrent tumor, including primary site recurrence, regional lymph node metastasis, and distant metastasis.

Correlation of radiomic features with SUVs

In this study, we selected a total of 38 radiomic features for further analysis **(Table 2)**. These features were selected based on comparison to the SUVs. The selected radiomic features displayed low correlations with the SUVs for shape, flatness, and some first-order features, potentially as a result of the size and location of the original NPC lesions. The Pearson's correlation analysis showed that the metabolic parameters had varying degrees of correlation with the selected radiomic features.

Construction of the prognosis prediction model

This study used the SVM algorithm to perform further feature selection, after which the Matlab- constructed model was used for validation and testing. The calculated results are as follows.

The best performing model was the SVM Kernel, which had an accuracy of 74.3%, a sensitivity of 95.9%, a specificity of 76.2% for the validation group, and an accuracy of 58.3%, a sensitivity of 91.7%, and a specificity of 75% for the test group.

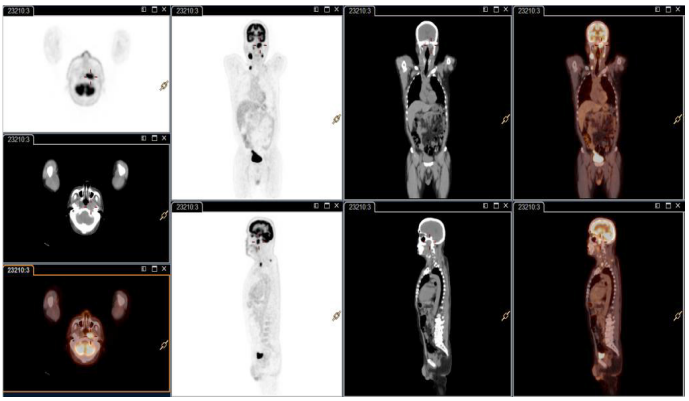

Figure 1: When selecting the ROI, the primary NPC site was set as local, which is defined as the area of high uptake area in the nasopharyngeal region on the PET image.

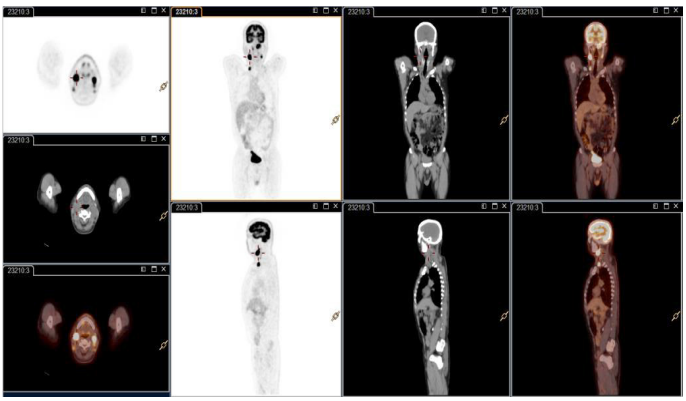

Figure 2: The primary site lymph node, set as Lymph X (where X represents a numerical code), was defined as the area of high lymph node uptake in the head and neck regions on PET images.

Table 1: Summarized data of all NPC patients.

	Validation	Test	statistic	p-value
Sample size	70	24	N/A	N/A
Age (years, mean ±SD)	53.56 ± 3	47.38 ± 0.5	2.086	0.0432
Gender (male/female)	50/20	16/8	-0.424	0.674
SUVmax	9.67 ± 4.82	10.8 ± 3.31	0.1794	0.858

Table 2: Correlation of radiomic features and SUV. Compared to SUVs, the radiomic features showed low correlation in shape, flatness, and some first-order features. The Pearson's correlation analysis showed that the metabolic parameters had varying degrees of correlation with the selected radiomic features. We selected the two most relevant radiomic features, Imc1_GLCM and Skewness_First Order, from local NPC lesions.

Radiomic feature	Correlation coefficient with SUVmax	Formula
Sphericity_Shape	0.055	$sphericity = \frac{\sqrt[3]{36\pi v^2}}{A}$
Elongation_Shape	0.127	$\text{elongation} = \sqrt{\frac{\lambda \min or}{\lambda major}}$
GrayLevelNonUniformity_GLDM	0.091	$\text{GLN} = \frac{\Sigma_{i=1}^{N_g}\Sigma_{j=1}^{N_d} p(i,j)\, j^2}{N^2}$
SmallDependenceEmphasis_GLDM	0.159	$\text{SDE} = \frac{\Sigma_{i=1}^{N_g}\Sigma_{j=1}^{N_d} \frac{P(i,j)}{i^2}}{N^2}$
Dependence Non Uniformity Normalized_GLDM	0.192	$\text{DNN} = \frac{\Sigma_{j=1}^{N_d}(\Sigma_{i=1}^{N_g} P(i,j))^2}{N^2}$
Large Dependence Emphasis_GLDM	-0.042	$\text{LDE} = \frac{\Sigma_{i=1}^{N_g}\Sigma_{j=1}^{Nd} P(i,j)\, j^2}{N^2}$
Large Dependence Low Gray Level Emphasis_GLDM	-0.042	$\text{LDLGLE} = \frac{\Sigma_{i=1}^{Ng}\Sigma_{j=1}^{Nd} \frac{p(i,j)\, j^2}{i^2}}{N^2}$
Dependence Variance_GLDM	-0.071	$\text{DV}=\sum_{i=1}^{Ng}\Sigma_{j=1}^{N_d} P(i.j)(j-u)^2$ $where\ \mu = \sum_{i=1}^{Ng}\Sigma_{j=1}^{N_d}\ \text{jp(i,j)}$
LowGray Level Emphasis_GLDM	0.156	$\text{LGLE} = \frac{\Sigma_{i=1}^{N_g}\Sigma_{j=1}^{Nd} \frac{p(i,j)}{i^2}}{N_Z}$
Maximum Probability_GLCM	0.165	$\text{maximum probability} = \max(\text{p(i,j)})$
Joint Energy_GLCM	-0.163	$\text{joint energy} = \sum_{i=1}^{N_g}\Sigma_{j=1}^{N_d}(P(i,j))^2$
Idn_GLCM	0.090	$\text{IDN} = \sum_{k=0}^{Ng-1} \frac{p_{x-y(k)}}{1+\left(\frac{k}{Ng}\right)}$
Idm_GLCM	-0.145	$\text{IDM} = \sum_{k=0}^{Ng-1} \frac{P_{x-y}(k)}{1+k\wedge 2}$
MCC_GLCM	-0.088	$\text{MCC}=\sqrt{\text{sec}\, ond\ \ l\,\text{arg}\, est\ \ eigenvalue\ of\ \ Q}$ $Q(i,j) = \Sigma_{k=0}^{N_g} \frac{P(i,k)P(j,k)}{P_z(i)P_y(k)}$

Imc2_GLCM	0.139	$\mathrm{IMC2} = \sqrt{1 - e^{-2(HXY2 - HXY)}}$
Imc1_GLCM	-0.103	$\mathrm{IMC1} = \frac{HXY - HXY1}{\max\{HX, HY\}}$
Id_GLCM	-0.155	$\mathrm{ID} = \Sigma_{k=0}^{Ng-1} \frac{px - y(k)}{1+k}$
Uniformity_First Order	-0.157	$\mathrm{uniformity} = \Sigma_{i=1}^{N_g} p(i)^2$
Minimum_First Order	-0.020	$\mathrm{minimum} = \min[\mathrm{X}]$
Percentile_10_First Order	0.134	The 10^{th} percentile of X
Kurtosis_First Order	0.107	$\mathrm{kurtosis} = \frac{\mu_4}{\sigma_4} = \frac{\frac{1}{Np}\Sigma_{i=1}^{Np} l \times \left(1^y - \bar{x}\right)^4}{\left(\left(\frac{1}{Np}\Sigma_{\pi=1}^{Np} Cx,i\right) - x_J^{-2}\right)^2}$
Low Gray Level Run Emphasis_GLRLM	-0.156	$\mathrm{LGLRE} = \frac{\Sigma_{i=1}^{N_g}\Sigma_{j=1}^{Nr} \frac{P(i,j\mid\theta)}{i^2}}{Nr(\theta)}$
Gray Level Non Uniformity Normalized_GLRLM	-0.156	$\mathrm{GLNN} = \frac{\sum_{i=1}^{N_g}\left(\Sigma_{j=1}^{N_r} P(i,j\mid\theta)\right)^2}{N_r(\theta)^2}$
Run Variance_GLRLM	0.049	$RV = \sum_{i=1}^{Ng}\sum_{j=1}^{Nr} P(i,j/\theta)(j-\mu)^2$
Gray Level Non Uniformity_GLRLM	0.050	$GLN = \frac{\sum_{i=1}^{Ng}\left(\Sigma_{j=1}^{N_r} P(i,j\mid\theta)\right)}{N_r(\theta)}$
Long Run Emphasis_GLRLM	0.041	$LER = \frac{\sum_{i=1}^{Ng}\Sigma_{j=1}^{Nr} P(i,j/\theta)j^2}{Nr(\theta)}$
Short Run Emphasis_GLRLM	0.084	$SRE = \frac{\sum_{i=1}^{Ng}\Sigma_{j=1}^{Nr} \frac{P(i,j/\theta)}{j^2}}{Nr(\theta)}$
Run Percentage_GLRLM	0.082	$RP = \frac{Nr(\theta)}{N_p}$
Long Run Low Gray Level Emphasis_GLRLM	0.029	$LRLGLRE = \frac{\sum_{i=1}^{N_g}\Sigma_{j=1}^{N_r} \frac{P(i_j j\mid\theta)\, j^2}{i^2}}{N_r(\theta)}$
Run Length Non Uniformity Normalized_GLRLM	0.099	$RLNN = \frac{\sum_{j=1}^{Nr}(\Sigma_{i=1}^{Ng} P(i,j\mid\theta))^2}{Nr(\theta)^2}$

Gray Level Non Uniformity Normalized_GLSZM	0.156	$GLNN = \frac{\sum_{i=1}^{N_g}(\Sigma_{j=1}^{N_s} p(i,j))^2}{N_Z^2}$
Large Area Emphasis_GLSZM	0.149	$LAE = \frac{\sum_{i=1}^{N_g}\Sigma_{j^{\Xi}1}^{Ns} p(i.j)j^2}{N_z}$
Zone Percentage_GLSZM	0.149	$ZP = \frac{N_z}{Np}$
Large Area Low Gray Level Emphasis_GLSZM	0.149	$LALGLE = \frac{\sum_{i=1}^{N_g}\Sigma_{j=1}^{Ns}\frac{P(i,j)i^2}{j^2}}{N_z}$
Small Area Emphasis_GLSZM	0.149	$SAE = \frac{\sum_{i=1}^{Ng}\Sigma_{j=1}^{Ns}\frac{P(i,j)}{j^2}}{N_z}$
Low Gray Level Zone Emphasis_GLSZM	-0.156	$LGLZE = \frac{\sum_{i=1}^{Ng}\Sigma_{j=1}^{Ns}\frac{P(i,j)}{i^2}}{N_z}$
Coarseness_NGTD	-0.138	$Coarseness = \frac{1}{\Sigma_{i=1}^{Ng} p_i s_i}$
Contrast_NGTDM	0.009	$Contrast = \left(\frac{1}{N_{g,p}(N_{g,p}-1}\sum_{i=1}^{Ng}\sum_{j=1}^{N_g} P_i P_j (i-j)^2\right)\left(\frac{1}{N_{v,p}}\sum_{j=1}^{Ng} Si\right), where\ Pi \neq 0, Pj \neq 0$

Discussion

After selecting the radiomic features most relevant to local NPC lesions from F-18 FDG PET images, we discussed the correlations between the radiomic features and the SUVs. The clinical value of the radiomic model in evaluating NPC stage was also analyzed. The results showed that there was a considerable correlation between the metabolic parameters and selected radiomic features.

Burri et al. [18] found that using 40% of the SUVmax of the PET image as the boundary of the lesion resulted in the best correlation with pathological and physiological characteristics of the tumor. As such, we decided to base our study on this method and measure metabolic parameters. The metabolic parameters of primary NPC represent the clinical parameters of tumor function, but the uptake of F-18 FDG does not always accurately reflect the physiological state of the tumor [19].

In this study, we used the level tracking [21] and PET Tumor Segmentation [22] tools to select ROIs for further analysis. These methods were based on imaging density, such as the histogram. The edge detection algorithm was also applied to segmentation methods. Like Burri et al. [18], the purpose of setting 40% of the SUVmax as the lesion boundary was in part to establish simple, accurate, and reproducible methods of ROI selection, and to ensure that the selected ROI included as much of the high uptake area as possible.

In recent years, increasingly prevalent evidence has shown that the radiomic analysis of medical images can better reflect potential spatial variation and heterogeneity of endosomal tumor intensity, which can generate more predictive and prognostic information [13, 24]. Du et al. [16] used machine learning methods to analyze post-therapy NPC PET/CT images and found that in differentiating between local tumor recurrence and inflammation, radiomics signatures showed higher AUC values as compared to conventional indicators (0.867–0.892 vs. 0.817), We used image features based on local NPC lesions from pretherapy PET images to assess its value in NPC staging. In this study, the best performing model was the SVM Kernel, which gave an accuracy of 74.3%, a sensitivity of 95.9%, and a specificity of 76.2% in the validation group, as well as an accuracy of 58.3%, a sensitivity of 91.7%, and a specificity of 75% in the test group. These results show high predictive efficacy for prognosis of NPC treatment response.

In this study, we selected a total of 38 radiomic features for further analysis **(Table 2)**. These radiomic features were selected based on a low correlation with SUVmax. The selected radiomic features displayed low correlations with the SUVs for

shape, flatness, and some first-order features, which may have been a result of the size and location of the original tumor in the selected NPC patients. The range of stages was T1~T2, and no patients displayed any distal metastases; therefore, the selected radiomic features displayed high correlation with tumor morphology. The Pearson's correlation analysis showed that the metabolic parameters had varying degrees of correlation with the selected radiomic features.

Despite the promising results, there were several limitations present in our study. First, the distribution of FDG in the body varies with respect to physiological period, which may affect the quality of the PET data to a certain extent. Retrospective collection of patient data was beneficial in that it allowed us to collect as much data as possible; however, the screening process was highly time- consuming, which resulted in a data pool smaller than what would have been ideal. In the future, we plan to carry out stricter standardization during the data preprocessing phase, similar to prospective methods. thereby allowing us to collect data from NPC patients satisfying the patient screening criteria.

Secondly, the sample size of this study was relatively small and all cases were collected from a single source. Both a larger sample size and multicenter evaluation are needed for verification of our results. In future NPC studies, we plan to build models based on a combination of radiomic features and PET parameters, as well as supplement our models by using external validation.

Thirdly, the Taichung Veterans General Hospital PET scanner was replaced in late 2020. The new PET scanner was equipped with a different detector and different reconstruction methods from the new era PET/CT. This replacement may have affected the radiomic feature results in the NPC patients who had their examinations performed in the new PET/CT scanner [23].

Conclusion

F-18 FDG PET is widely used for cancer screening and post-treatment evaluation because of its high sensitivity, but its low specificity makes it difficult to distinguish the high uptake areas of NPC recurrence and second cancer. A delayed scan is also necessary in order to figure out the radiation inflammatory response after radiotherapy or the real tumor lesion.

For ROI selection, we used a semi-automatic drawing method to ensure the reproducibility of the ROI by different operators. Compared with the workstation provided by the PET/CT scanner manufacturer, the semi-automatic selection method is more time-intensive and requires modification to the ROI after selection.

This experiment only used the PET images from PET/CT studies. It was mentioned by Lv et al. in 2019 that in addition to PET images, CT images can be used in combination for radiomic feature extraction and screening [24]. In addition, other studies have discussed the use of a nomogram [25] or weighted radscore calculation method [26] in obtaining more information beneficial to the processes of clinical diagnosis and treatment.

In this study, we found that radiomic features selection and modeling in PET images can increase the accuracy of prognosis prediction for NPC patients. In our future work, we hope to create a prediction model for NPC and perform validation of our clinical PET images.

References

1. Sung H, Ferlay J, Siegel RL, Laversanne M, Soerjomataram I, et al. Global Cancer Statistics 2020: GLOBOCAN Estimates of Incidence andMortality Worldwide for 36 Cancers in 185 Countries. CA Cancer J Clin. 2021; 71: 209-249.
2. Tang LL, Chen WQ, Xue WQ, He YQ, Zheng RS, Zeng YX, et al. GlobalTrends in Incidence and Mortality of Nasopharyngeal Carcinoma. Cancer Lett. 2016; 374: 22-30.
3. Wei KR, Zheng RS, Zhang SW, Liang ZH, Li ZM, et al. Nasopharyngealcarcinoma incidence and mortality in China, 2013. Chin J Cancer. 2017; 36: 90.
4. Chua DTT, Wei WI, Wong MP, Sham JST, Nicholls J, et al. Phase II study of gefitinib for the treatment of recurrent and metastatic nasopharyngeal carcinoma. Head Neck. 2008; 30: 863-867.
5. Hsieh JCH, Hsu CL, Ng SH, Wang CH, Lee KD, et al. Gemcitabine plus cisplatin for patients with recurrent or metastatic nasopharyngeal carcinoma in Taiwan: a multicenter prospective Phase II trial. Jpn J Clin Oncol. 2015; 45: 819-827.
6. Lin J, Xie G, Liao G, Wang B, Yan M, et al. Prognostic value of 18F-FDG-PET/CT in patients with nasopharyngeal carcinoma: a systematic review and meta-analysis. Oncotarget. 2017; 8: 33884-33896.
7. Hsieh TC, Hsieh CY, Yang TY, Chen TT, Lin CY, et al. [18F]-Fluorodeoxyglucose positron emission tomography standardized uptake value as a predictor of adjuvant chemotherapy benefits in patients with nasopharyngeal carcinoma. Oncologist. 2015; 20: 539-545.
8. Aktan M, Kanyilmaz G, Yavuz BB, Koc M, Eryilmaz MA, et al. Prognostic value of pre-treatment 18F-FDG PET uptake for nasopharyngeal carcinoma. Radiol Med. 2017.
9. Connor JPB, Rose CJ, Waterton JC, Carano RAD, Parker GJM, et al. Imaging Intratumor Heterogeneity: Role in Therapy Response, Resistance, and Clinical Outcome. Clin Cancer Res. 2015; 21: 249.
10. Davnall F, Yip CS, Ljungqvist G, Selmi M, Ng F, et al. Assessmentof Tumor Heterogeneity: An Emerging Imaging Tool for Clinical Practice?Insights Imaging. 2012; 3: 573-589.
11. Weidong Wang JL. Reflection and prospect: precise radiation therapy based onbio-omics/radiomics and artificial intelligence technology. Chin J Clin Oncol. 2018; 45: 604-608.
12. Zhang B, Ouyang F, Gu D, Dong Y, Zhang L, et al. Advanced nasopharyngeal carcinoma: pre-treatment prediction of progression based on multi-parametric MRI radiomics. Oncotarget. 2017; 8: 72457-72465.
13. Zhang B, Tian J, Dong D, Gu D, Dong Y, et al. Radiomics features of multiparametric MRI as novel prognostic factors in advanced nasopharyngeal carcinoma. Clin Cancer Res. 2017; 23: 4259-4269.
14. SararasIntarak, Yuda Chongpison, Mananchaya Vimolnoch, Sornjarod Oonsiri, Sarin Kitpanit, Anussara Prayongrat, et al. Tumor Prognostic Prediction of Nasopharyngeal Carcinoma Using CT-Based Radiomics in Non-Chinese Patients. Front Oncol. 2022; 12: 775248.
15. Ming X, Oei RW, Zhai R, Kong F, Du C, et al. MRI-Based RadiomicsSignature Is a Quantitative Prognostic Biomarker for NasopharyngealCarcinoma. Sci Rep. 2019; 9: 10412.
16. Giraud P, Giraud P, Gasnier A, El Ayachy R, Kreps S, et al. Radiomicsand Machine Learning for Radiotherapy in Head and Neck Cancers. Front Oncol. 2019; 9: 174.

17. Zeng C, Zhai T, Chen J, Guo L, Huang B, et al. Imaging Biomarkers ofContrast-Enhanced Computed Tomography Predict Survival in OesophagealCancer After Definitive Concurrent Chemoradiotherapy. Radiat Oncol. 2021; 16: 8.

18. Burri RJ, Rangaswamy B, Kostakoglu L, Hoch B, Genden EM, et al. Correlation of positron emission tomography standard uptake value and pathologic specimen size in cancer of the head and neck. Int J Radiat Oncol Biol Phys. 2008; 71: 682-688.

19. Mac Manus MP, Ding Z, Hogg A, Herschtal A, Binns D, et al. Association between pulmonary uptake of fluorodeoxyglucose detected by positron emission tomography scanning after radiation therapy for non–small-cell lung cancer and radiation pneumonitis. Int J Radiat Oncol Biol Phys. 2011; 80: 1365-1371.

20. Wenyue Duan, Bingdi Xiong, Ting Tian, Xinyun Zou, Zhennan He, et al. Radiomics in Nasopharyngeal Carcinoma. Clin Med Insights Oncol. 2022; 16: 1-10.

21. Cs. Pinter, A. Lasso, G. Fichtinger. Polymorph segmentation representation for medical image computing", Computer Methods and Programs in Biomedicine. 2019; 171: 19-26.

22. Beichel RR, M. Van Tol, EJ Ulrich, C Bauer, T Chang, et al. "Semi-automated Segmentation of Head and Neck Cancers in 18F-FDG PET Scans: A Just-Enough-Interaction Approach", in Medical Physics, 2016.

23. Altazi BA, Zhang GG, Fernandez DC, Montejo ME, Hunt D, et al. Reproducibility of F18-FDG PET radiomic features for different cervical tumor segmentation methods, gray-level discretization, and reconstruction algorithms. J Appl Clin Med Phys. 2017; 18: 32-48.

24. Lv W, Yuan Q, Wang Q, Ma J, Feng Q, et al. "Radiomics analysis of PET and CT components of PET/CT imaging integrated with clinical parameters: application to prognosis for nasopharyngeal carcinoma." Molecular Imaging and Biology. 2019; 21: 954-964.

25. Gu B, Gu B, Zhang J, Ma G, Song S, Shi L, et al. "Establishment and validation of a nomogram with intratumoral heterogeneity derived from 18F-FDG PET/CT for predicting individual conditional risk of 5-year recurrence before initial treatment of nasopharyngeal carcinoma." BMC cancer. 2020; 20: 1-12.

26. Feng Q, Liang J, Wang L, Niu J, Ge X, et al. "Radiomics analysis and correlation with metabolic parameters in nasopharyngeal carcinoma based on PET/MR imaging." Frontiers in oncology. 2020; 10: 1619.